Durham University

Durham Research Online

Deposited in DRO:

01 August 2016

Version of attached file:

Accepted Version

Peer-review status of attached file:

Peer-reviewed

Citation for published item:

Goulty, N.R. and Sargent, C. and Andras, P. and Aplin, A.C. (2016) 'Compaction of diagenetically altered mudstones - Part 1 : mechanical and chemical contributions.', Marine and petroleum geology., 77 . pp. 703-713.

Further information on publisher's website:

http://dx.doi.org/10.1016/j.marpetgeo.2016.07.015

Publisher's copyright statement:

© 2016 This manuscript version is made available under the CC-BY-NC-ND 4.0 license
http://creativecommons.org/licenses/by-nc-nd/4.0/

Additional information:

Use policy

The full-text may be used and/or reproduced, and given to third parties in any format or medium, without prior permission or charge, for personal research or study, educational, or not-for-profit purposes provided that:

- a full bibliographic reference is made to the original source
- a link is made to the metadata record in DRO
- the full-text is not changed in any way

The full-text must not be sold in any format or medium without the formal permission of the copyright holders.

Please consult the full DRO policy for further details.

Durham University Library, Stockton Road, Durham DH1 3LY, United Kingdom
Tel : +44 (0)191 334 3042 | Fax : +44 (0)191 334 2971
https://dro.dur.ac.uk

Compaction of diagenetically altered mudstones – Part 1: Mechanical and chemical contributions

N.R. Goulty*, C. Sargent, P. Andras, A.C. Aplin

Department of Earth Sciences, Durham University, South Road, Durham DH1 3LE, UK

*Corresponding author.

E-mail address: n.r.goulty@durham.ac.uk (Neil Goulty).

Marine and Petroleum Geology, **77**, 703-713 (published online 26 July 2016).

DOI: 10.1016/j.marpetgeo.2016.07.015

Abstract

At low temperatures, siliciclastic mudstones compact mechanically. Above 70 °C, where the smectite-to-illite transformation dominates clay diagenesis, they also compact chemically, provided that excess pore water can escape. There are two prevailing conceptual models for the compaction of siliciclastic mudstones at higher temperatures, above ~100 °C. One holds that precipitation of minerals during diagenesis cements the mudstones such that mechanical compaction no longer occurs even if the mudstones can drain freely. According to the other model, diagenetically altered mudstones continue to compact mechanically in response to increasing effective stress. We found that wireline-log and pressure data from Cretaceous mudstones at Haltenbanken are consistent with ongoing mechanical compaction accompanying chemical compaction up to at least 130 °C. We suggest that mechanical compaction continues because grain contacts in siliciclastic mudstones following smectite-to-illite transformation are still mostly between clay grains.

Keywords: Mudstone; Clay diagenesis; Chemical compaction; Mechanical compaction; Overpressure; Effective stress

Highlights

- We investigated compaction hypotheses for diagenetically altered mudstones.
- The study used well data from Cretaceous formations at Haltenbanken.
- Overpressure is due to disequilibrium compaction and clay diagenesis.
- Mechanical compaction continues up to temperatures of at least 130 °C.
- The hypothesis that mudstones only compact chemically above 100 °C is falsified.

1. Introduction

Muds and mudstones are the world's most common sediment type (Schieber, 1998). Knowledge of their compaction behaviour is essential for pre-drill pore pressure estimation from basin modelling and seismic velocities. Relationships between wireline log responses and effective stress are also required for estimating pore pressure while drilling through mudstone formations, to anticipate the pore pressures that will be encountered when the drill-bit encounters permeable reservoir formations. These two articles on compaction and overpressure in diagenetically altered mudstones are directed towards improved pore pressure estimation using wireline logs in mudstones at the temperatures where clay diagenesis takes place. Here, in Part 1, we discriminate between two alternative hypotheses concerning compaction processes in diagenetically altered mudstones, and in Part 2 (Goulty and Sargent, 2016) the implications for pore pressure estimation are explained.

In the conversion of muds to mudstones during burial, mechanical compaction dominates initially, with grains becoming more closely packed together through slippage, rotation and breakage. Provided that potassium is available, commonly sourced by the dissolution of potassium feldspar, transformation of smectite to illite starts at around 65–70 °C and is the principal clay diagenetic change in mudstones up to ~120 °C. The reaction pathways release water, silica and cations that can react with kaolinite and calcite to produce chlorite and ankerite (Boles and Franks,

1979). In addition, most detrital plagioclase becomes albitized as a result of reacting with sodium ions released from the transforming smectite (Milliken 1992). When mudstones have attained a temperature of ~120 °C through burial, the proportion of expandable 'smectitic' interlayers containing hydrated cations in mixed-layer illite/smectite crystals has generally reduced to about 20 % with all the smectite 2:1 layers having dissolved, so that the remaining expandable interlayers separate illite fundamental particles (Środoń et al., 2000). Details of other diagenetic reactions that take place in mudstones in the temperature range 70–120 °C are given by Hower et al. (1976), Freed and Peacor (1989), Bjørlykke (1998), Nadeau et al. (2002), Nadeau (2011) and Thyberg and Jahren (2011). Above 120 °C, kaolinite starts to transform to illite, provided that potassium is still available, with further release of water (Giorgetti et al., 2000; Nadeau et al., 2002).

According to Bjørlykke and Høeg (1997), compaction of mudstones at depths greater than 2–3 km is mainly chemical, involving dissolution and precipitation of minerals, and Bjørlykke (1998) stated that mudstones with overpressures at depths where chemical compaction is dominant (> 2–3 km depth, > 70–100 °C) should not be expected to have significantly higher porosity than normally pressured rocks. Their conceptual model is summarized on the left side of Fig. 1. Following the initial stage where mechanical compaction dominates, there is a transitional stage in which chemical compaction due to clay diagenesis has started and mechanical compaction continues. Chemical compaction dominates at higher temperatures, and by implication proceeds independently of effective stress.

An alternative conceptual model for the compaction of diagenetically altered mudstones was set out by Dutta (2002), who had previously modelled mudstone compaction and overpressure generation with the inclusion of reaction kinetics for the transformation of smectite to illite (Dutta, 1986). A key aspect of the model is the suggestion by Lahann (2002) that the normal compaction trend for a mudstone is bounded by distinct compaction profiles for smectite-rich mudstone and illite-rich mudstone, before and after the main phase of smectite-to-illite transformation. In this model, which is summarized on the right side of Fig. 1, the porosity of diagenetically altered

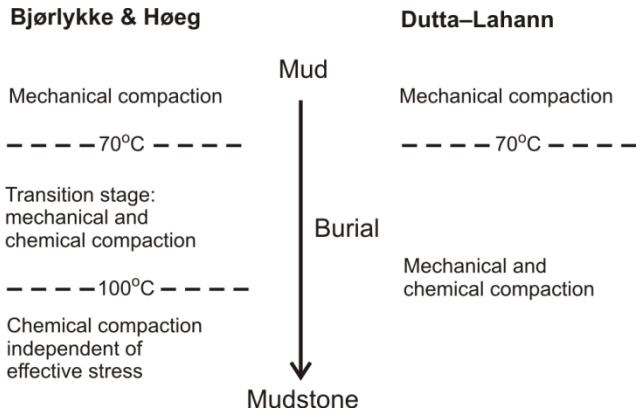

Fig. 1. Alternative conceptual models for the compaction of mudstones. Left: the model of Bjørlykke and Høeg (1997) and Bjørlykke (1998), in which mudstones at temperatures above ~100 °C compact chemically, independent of effective stress. Right: the model of Dutta (2002) and Lahann (2002) in which mechanical compaction continues together with chemical compaction in diagenetically altered mudstones.

mudstones depends on both effective stress and temperature history, and there is no suggestion that mechanical compaction becomes negligible at temperatures above ~100 °C.

We have investigated Cretaceous mudstones in the Haltenbanken area, offshore mid-Norway (Fig. 2) at depths where temperatures are in the range 70–170 °C. The sparse pressure data available in the Cretaceous formations show that the mudstones are overpressured with a fairly consistent pore pressure–depth profile across the area (O'Connor et al., 2012). We found large differences between compaction profiles and concluded that the vertical effective stress history was the principal factor responsible for the differences, even though the vertical effective stress shows little spatial variation at the present day (Cicchino et al., 2015). Sargent et al. (2015) analysed density and sonic logs together to show how the amount of overpressure due to unloading processes can be estimated from these logs.

Here we use the wireline-log and pressure data in Cretaceous mudstones at Haltenbanken to discriminate between the two conceptual models for mudstone compaction. Our results are consistent with the idea that mechanical compaction continues to occur in diagenetically altered mudstones subject to increasing effective stress; the results falsify the hypothesis that porosity in

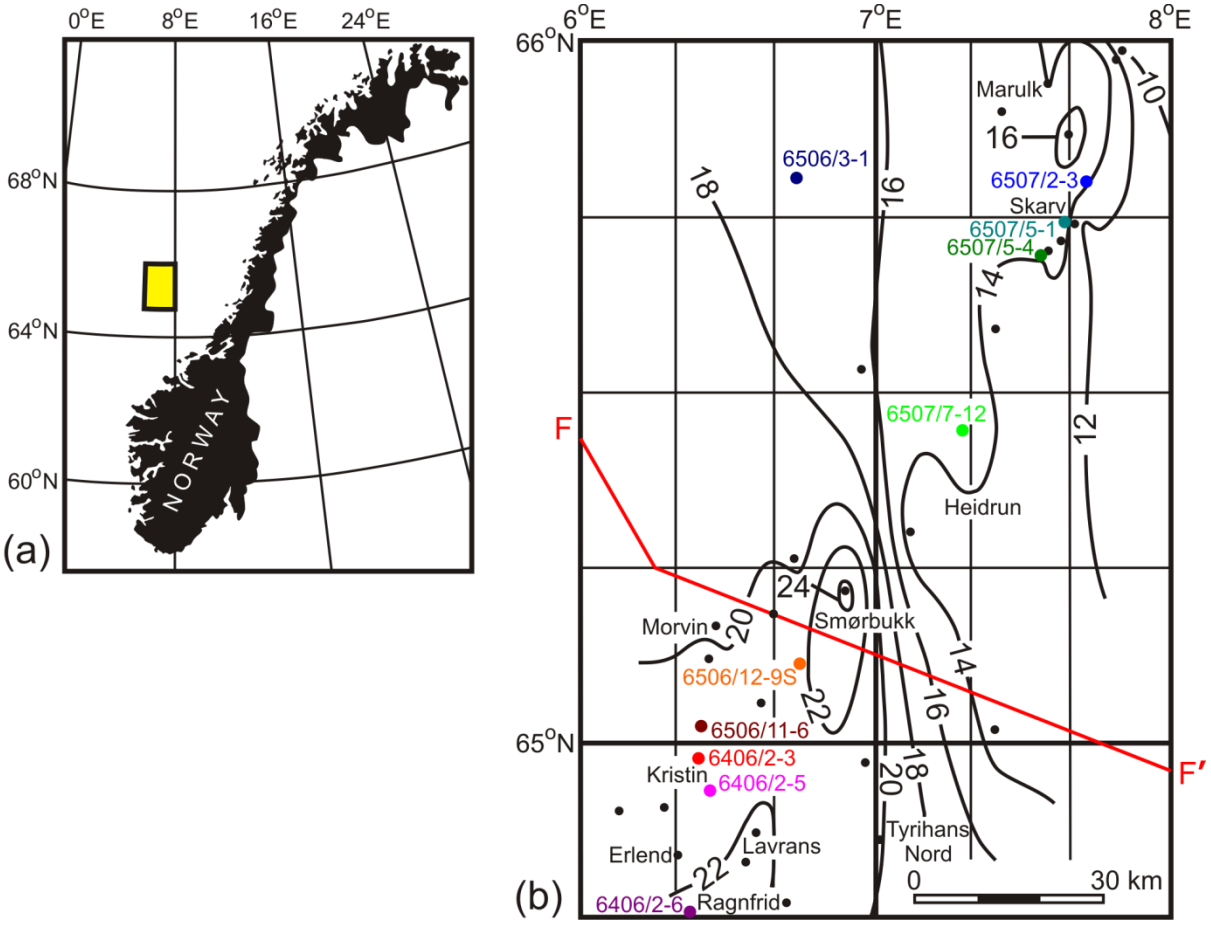

Fig. 2. (a) Location map of the study area, offshore mid-Norway. (b) Spatial variation of the density log porosity values (%) on the best-fitting exponential trends for the Kvitnos and Lange mudstones at 2700 m depth below seafloor. Crooked line FF' marks the location of the geoseismic section shown in Fig. 4.

mudstones undergoing diagenesis at temperatures above 100 °C is a function only of chemical processes and independent of effective stress.

2. Compaction profiles for Cretaceous mudstones at Haltenbanken

Within Cretaceous mudstones in the Haltenbanken area, offshore mid-Norway, Cicchino et al. (2015) found substantial lateral variations in porosity, contoured in Fig. 2b, in spite of the fact that the pressure–depth profile within the Cretaceous formations is fairly consistent across the area (Fig. 3). In this section, we summarize the geological background, the interpreted pore pressure history, and the density data from which mudstone porosity was inferred.

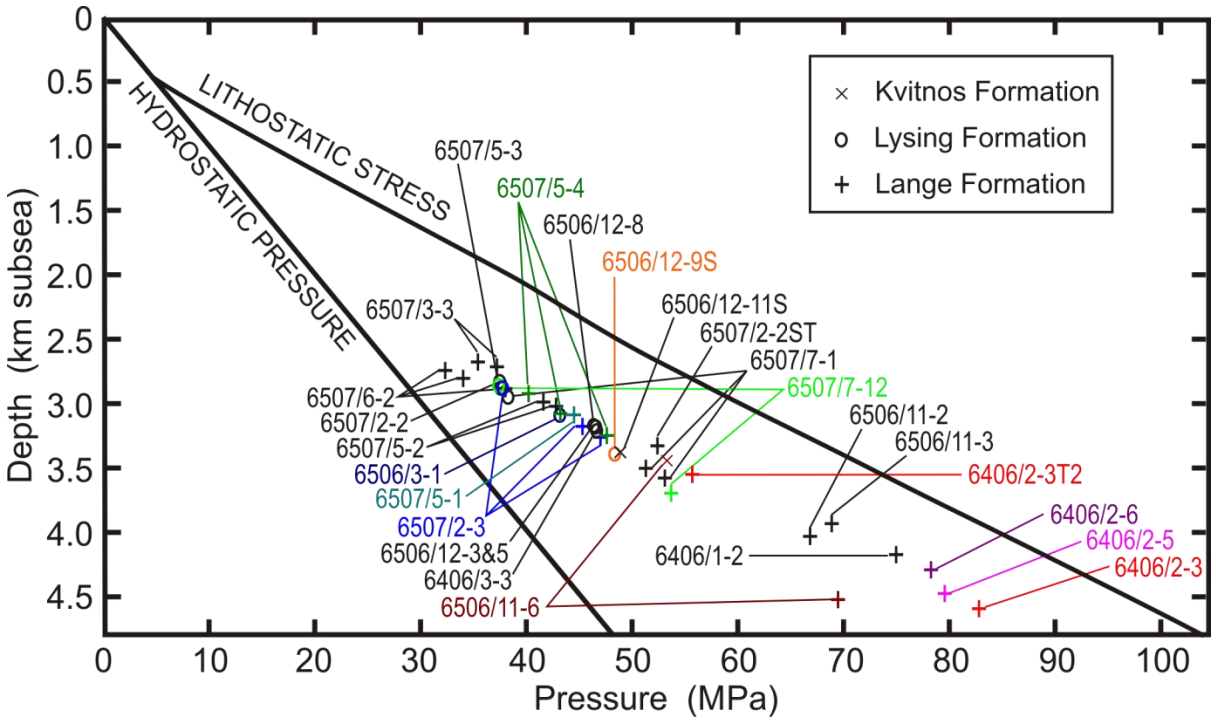

Fig. 3. Multi-well pressure–depth plot showing pressure measurements from isolated turbidite sandstone bodies within the Cretaceous formations (after O'Connor *et al*. 2012). The deeper pressure measurement in well 6506/11-6 is in the lowest acceptable category for data quality (O'Connor et al., 2012), and is probably erroneous because it is out of line with measurements in neighbouring wells. The lithostatic stress is an average profile for the wells with good density logs.

2.1. Geological background

The Halten Terrace (Fig. 4) is a structure that developed during a Jurassic–Early Cretaceous rift episode, bounded by the Klakk and Bremstein fault complexes (Blystad et al., 1995). The Cretaceous post-rift sediments are dominated by the mudstone lithology of the relatively deep marine palaeo-environment. Mudstones of the Lange Formation dominate the Lower Cretaceous succession and extend upwards into the Upper Cretaceous, where they are overlain by the clay-rich Kvitnos Formation (Dalland et al., 1988). The Lange and Kvitnos formations form the study interval, with a combined thickness that comprises about 75% of the Cretaceous strata in the area. The Lange Formation has a maximum recorded thickness of about 1300 m at Haltenbanken. There are a few stringers of limestone in the lower part of the formation and several sandstone turbidite bodies, generally isolated and encased in mudstone, in the upper part. These turbidites include the Lysing Formation where some of the pressure measurements (Fig. 3) were made, which is coeval with the

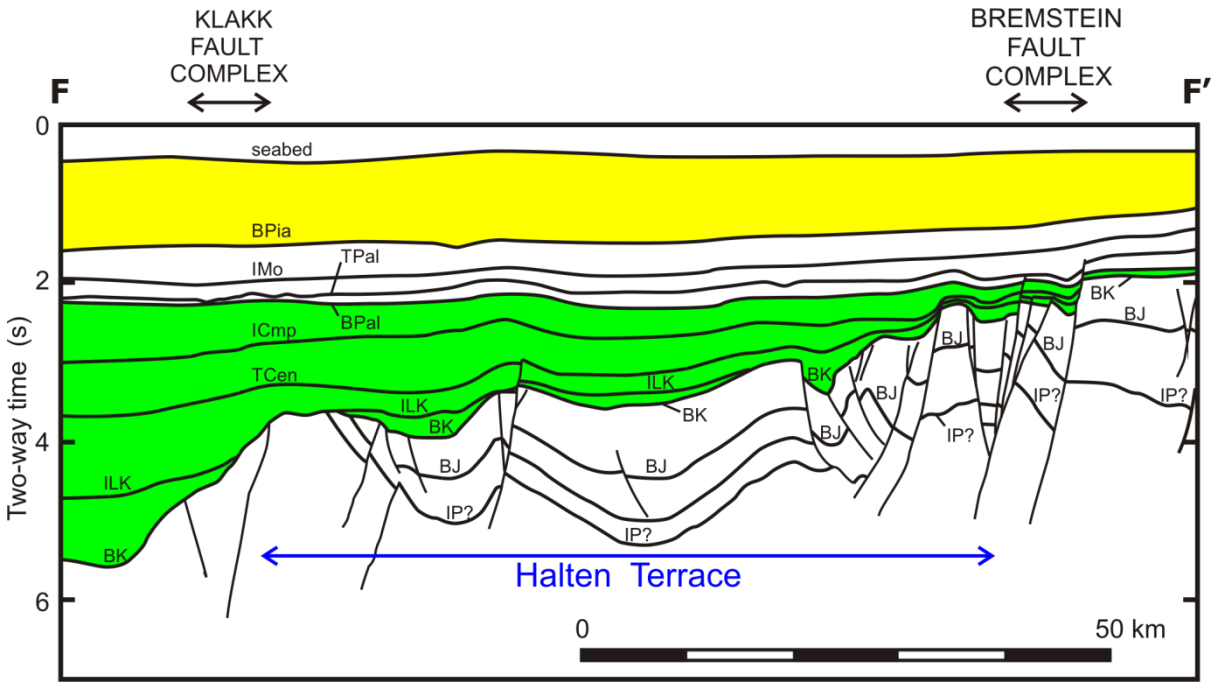

Fig. 4. Geoseismic section along profile FF' (see Fig. 2b for location). This figure corresponds to part only of geoseismic section FF' in Blystad et al. (1995). Key to picked horizons: BPia – Base Upper Pliocene; IMo – Intra-Miocene; TPal – Top Paleocene; BPal – Base Paleocene; ICmp – Intra-Campanian; TCen – Top Cenomanian; ILK – Intra-Lower Cretaceous; BK – Base Cretaceous; BJ – Base Jurassic; IP? – Intra-Permian(?). The Lange Formation lies between the Top Cenomanian and Base Cretaceous horizons. The Kvitnos Formation immediately overlies the Top Cenomanian horizon. After Blystad *et al*. (1995).

youngest Lange mudstones. The Kvitnos Formation is around 500 m thick and predominantly consists of claystones, interbedded with stringers of carbonate and sandstone.

The Kvitnos Formation is overlain by around 1200 m thickness of Upper Cretaceous, Palaeogene and Neogene claystone formations, terminating at an unconformity that developed during the late Pliocene (Dalland et al., 1988; Blystad et al., 1995). Between 2.8 Ma and the present, following the late Pliocene hiatus, glaciogenic sediments of the Naust Formation have been deposited in a series of east-to-west prograding wedges (Rise et al., 2005, 2006; Ottesen et al., 2009; Dowdeswell et al., 2010). Their thickness ranges up to 1300 m in the study area, so the deposition rate was much more rapid after 2.8 Ma than at any earlier time during the Cenozoic era (Fig. 4).

2.2. Pore pressure history and density logs

During mechanical compaction, increasing effective stress pushes the grains closer together as water escapes from the pore space, reducing porosity and permeability. When water cannot escape fast enough to remain in hydrostatic equilibrium as burial proceeds, overpressure is said to be generated by disequilibrium compaction. The retention of excess water necessarily means that the porosity is greater than it would be if the pore water were in hydrostatic equilibrium. Clay diagenesis can also generate overpressure. Illitization of smectite produces some water and makes a mudstone more compactable, so its density becomes greater at constant effective stress (Lahann, 2002). Again, overpressure is generated if pore water cannot escape fast enough to remain in hydrostatic equilibrium. A significant difference between disequilibrium compaction and clay diagenesis as mechanisms of overpressure generation is that clay diagenesis may increase the pore pressure sufficiently to reduce the effective stress acting on the mudstone, in which case the mudstone is said to be unloaded. Disequilibrium compaction acting alone in a mudstone bed cannot reduce the effective stress because no fluid expansion is involved, and the sediment framework does not become more compactable without diagenesis.

Skar et al. (1999) and O'Connor et al. (2012) suggested that the Cretaceous formations at Haltenbanken may have been hydrostatically pressured immediately prior to deposition of the Naust Formation, because the burial rate during the Cenozoic was slow before 2.8 Ma. The top of overpressure is encountered in the Palaeogene formations, where the overpressure has been attributed to disequilibrium compaction that resulted from the rapid deposition of the Naust Formation (Hermanrud et al., 1998; O'Connor et al., 2012). Pressure measurements in sandstones within the Cretaceous formations are sparse, although they are thought to be representative of the pressures in the mudstones because there is no evidence of lateral drainage through the sandstone bodies (O'Connor et al., 2012), such as marked reductions in overpressure along drainage pathways or shoulder effects on wireline logs. The measured pore pressures (Fig. 3) show that the pressure–depth profile has little lateral variation and is broadly parallel to the lithostatic stress.

If the pressure–depth profile of Fig. 3 is considered in isolation, without regard to other data, it might be inferred that overpressure had been generated by disequilibrium compaction. However, the geothermal gradient inferred from drill-stem tests is 36–40 °C km^{-1} (Cicchino et al., 2015), so the temperature at the depths of the shallowest pressure measurements in Fig. 3 are >90 °C. XRD results showed progressive illitization of mixed-layer illite/smectite with depth and confirmed that clay diagenesis is well under way at these depths (Cicchino et al., 2015). Furthermore, the density in Haltenbanken wells increases substantially with depth through the Kvitnos and Lange formations (Fig. 5a), implying that porosity strongly decreases with depth (Cicchino et al., 2015).

Skar et al. (1999) and O'Connor et al. (2012) attributed the Cretaceous overpressures to the combination of disequilibrium compaction, due to rapid burial since 2.8 Ma by the thick Naust sequence (Fig. 4), and clay mineral transformations. The absence of source rocks in the Cretaceous mudstones means that gas generation is unlikely to be a significant internal source of overpressure. The mudstones of the Kvitnos and Lange formations are all buried to depths where temperatures exceed 70 °C, so clay diagenesis is a viable mechanism for generating overpressure within them. In fact, most of the Cretaceous mudstones investigated here have reached temperatures above 100 °C, where one would expect porosity to be independent of effective stress according to the conceptual model of Bjørlykke and Høeg (1997) (Fig. 1).

The wide range of porosity–depth trends in Cretaceous mudstones at Haltenbanken is equivalent to a variation in porosity by a factor of two at a common depth of 2700 m below seafloor (Fig. 2b). Cicchino et al. (2015) investigated possible causes. They ruled out exhumation as the main cause of the lateral variation in compaction trends because the stratigraphic evidence from well and seismic data shows that the sediments are currently at their maximum burial depths across the area covered by Fig. 2b. They also ruled out variations in geothermal gradient as the main cause, because when porosities were plotted against temperature or against depth below the base of the Naust Formation, the range of porosity trends was only slightly reduced. Cicchino et al. (2015) reported

XRD results from four wells and and grain size analyses from two wells, and could not identify any lithological factor that might contribute significantly to the lateral variation in compaction trends.

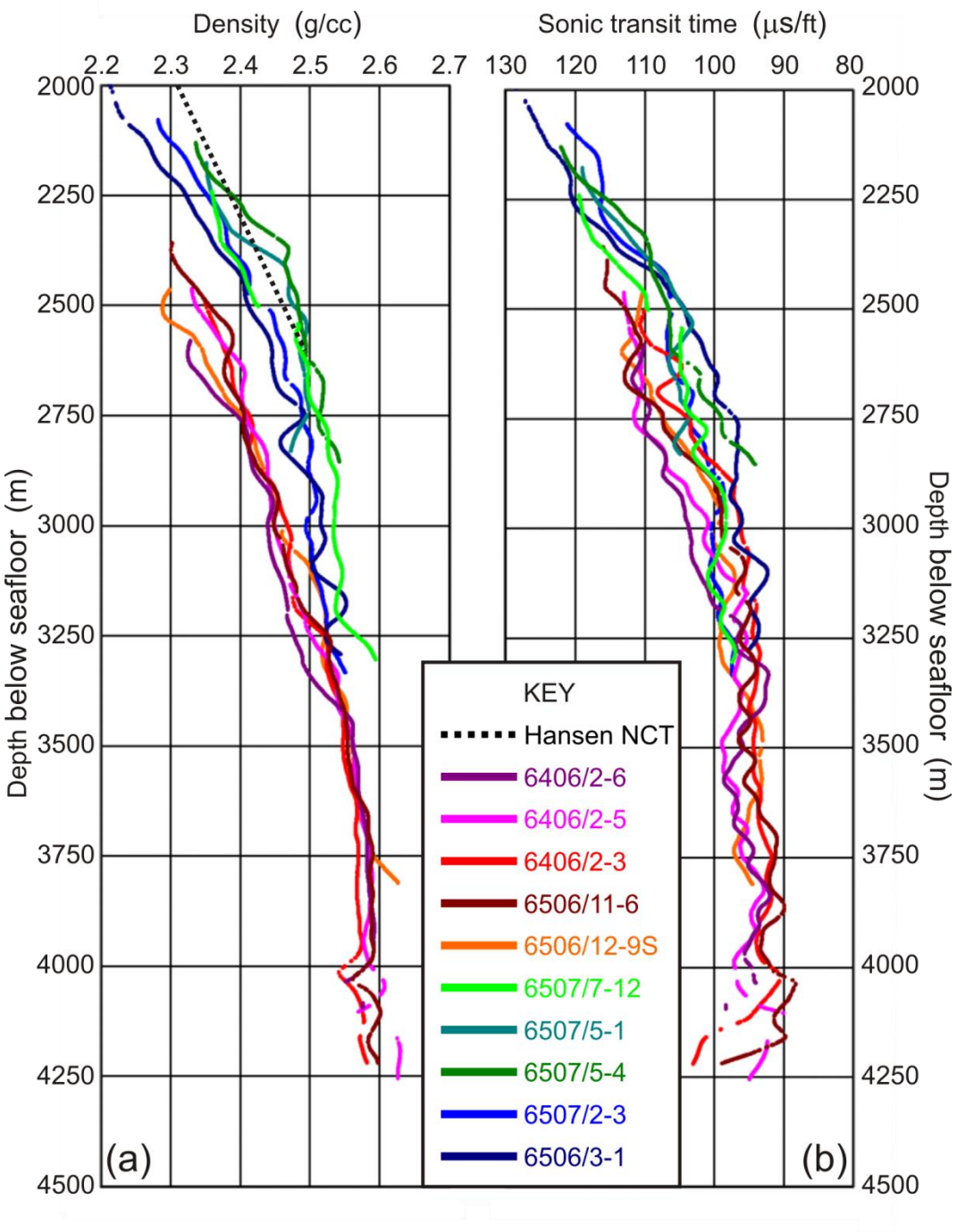

Fig. 5. Wireline logs through the Cretaceous Kvitnos and Lange formations in ten wells, plotted after selection of mudstone data points and smoothing: (a) density; and (b) sonic transit time. The linear porosity–depth trend of Hansen (1996) has been converted back into a depth trend here, using 2.75 g cm^{-3} for the density of the solid grains and 1.05 g cm^{-3} for the pore fluid.

Cicchino et al. (2015) compared the density–depth trends with the porosity–depth trend determined by Hansen (1996) for hydrostatically pressured Cretaceous and Tertiary mudrocks on the Norwegian Shelf (Fig. 5a) and inferred that the lower porosity mudstones at Haltenbanken are close to being normally compacted, even though they are now overpressured. Cicchino et al. (2015) interpreted the lateral variations in mudstone porosity as the result of lateral variations in the efficacy of water escape following rapid Naust burial, and suggested that the mudstones subsequently became better sealed by ongoing clay diagenesis and lithification. They also speculated that lateral variations in overpressure were greater in the early Pleistocene, following deposition of the majority of the Naust Formation. In the next section, we report further analysis that supports both these ideas.

3. Unloading and overpressure mechanisms

In this section, we establish depths to the onset of unloading in each well, and then relate lateral variations in these depths to lateral variations in effective stress history. In section 4, we explain how the lateral variations in effective stress history provide evidence that mechanical compaction continues in mudstones at depths where the temperature exceeds 100 °C. Unloading is best indicated on a sonic–density crossplot for mudstones of consistent lithology, so here we first review the application of these crossplots to identify where unloading mechanisms of overpressure generation are active in diagenetically altered mudstones. To improve the consistency of the trends on the crossplots, we introduce log-based corrections to the sonic logs to take account of variations in the clay content of the mudstones. Then we show crossplots for the Kvitnos and Lange formations in ten Haltenbanken wells and use them to interpret overpressure mechanisms.

3.1. Sonic–density crossplots

Crossplots of sonic transit time and density for analysing pore pressure in mudstones were introduced by Dutta (2002), although others had previously crossplotted velocity and density. The

curve marked with arrows in Fig. 6 approximates the average trend reported by Dutta (2002) for mudstones in the Gulf of Mexico. He identified a linear early compaction trend for smectite-rich mudstones and a linear late compaction trend for illite-rich mudstones, joined by a transitional section. The early compaction trend corresponds to the mechanical compaction stage for these smectite-rich muds and is similar to the Gardner trend for mud/mudstone (Gardner et al. 1974). In the transitional section, illitization of smectite has started while mechanical compaction is ongoing. The late compaction trend is similar to Bowers' (2001) lower velocity bound for mudstone; both apply for illite-rich mudstone.

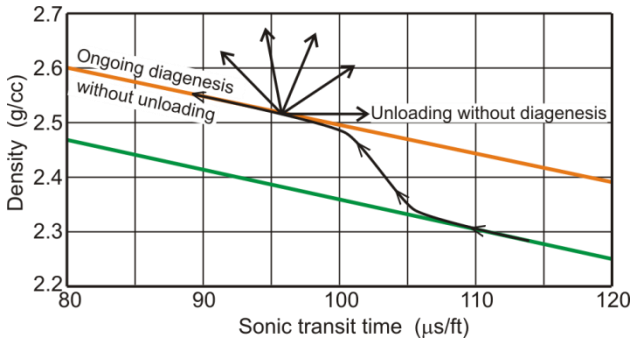

Fig. 6. Mudstone compaction trend (black arrowed curve) on a sonic–density crossplot based on results obtained by Dutta (2002) in the Gulf of Mexico. The trend is followed by mudstones undergoing progressive burial and compaction without unloading. The lower (green) and upper (orange) straight lines are Dutta's trends for smectite-rich and illite-rich mudstones, respectively. The fan of arrows indicates possible depth trends for a diagenetically altered mudstone, ranging from ongoing diagenesis without unloading to unloading without diagenesis.

Clay diagenetic reactions depend on both temperature and time, so the onset of the transitional section of the arrowed curve in Fig. 6 starts at ~70 ^{o}C and the linear late compaction trend typically starts at some temperature in the range 90–100 ^{o}C. Thus the transitional section is displaced to greater sonic travel time and lower density in basins with higher geothermal gradients or slower burial rates. Compaction trends on the sonic–density crossplot are also dependent on clay and silt content. For illite-rich mudstones, compaction trends exhibit higher transit times for a given density with increasing clay content (Katahara, 2003, 2006).

If disequilibrium compaction occurs in muds at the mechanical compaction stage, progress along the compaction trend is slowed, or even halted, because the normal reduction in porosity with depth is inhibited by the inability of pore water to escape and remain in hydrostatic equilibrium. Disequilibrium compaction may also occur after clay diagenesis has started. If the effective stress remains constant as clay diagenesis progresses, the density increases because clay diagenesis makes the mudstone more compactable (Lahann, 2002). For mudstones on the transitional section of the curve, we expect their trend on the crossplot to approach the late compaction trend for illite-rich mudstone at lower density. For illitized mudstones on the late compaction trend, we suggest that disequilibrium compaction would slow progress along that trend but not deviate from it.

If the effective stress acting on a mudstone decreases at any stage of compaction, the resulting effect on rock properties is to increase the sonic travel time and reduce the resistivity whilst having negligible effect on bulk density. Then the shift on the sonic–density crossplot would be towards the right. Bowers and Katsube (2002) suggested that this unloading behaviour occurs because the mudstone responds poroelastically to decreasing effective stress with flexible connecting pores of high aspect ratio opening by a very small amount, sufficient to affect the sonic velocity and resistivity while barely increasing the bulk porosity and barely changing the density. Unloading may be brought about by pore pressure increases, whether due to fluid influx caused by gas generation or lateral or vertical transfer, or due to clay diagenesis in mudstones which are so well sealed that pore water cannot escape. For illite-rich mudstones experiencing ongoing burial and diagenesis with water escape sufficiently inhibited for effective stress to decrease with increasing depth, the trend on the crossplot lies somewhere on the arc between the late compaction trend and the unloading response for no diagenesis (Fig. 6).

3.2. Crossplots for Cretaceous mudstones at Haltenbanken

Exploration wells were selected by Cicchino et al. (2015) where the top Kvitnos–base Lange interval is thicker than 300 m and both density and natural gamma logs had been recorded

throughout the interval. After quality control, these criteria yielded a set of 36 wells from the area shown in Fig. 2b, of which ten wells containing at least one direct measurement of pressure were selected by Sargent et al. (2015) in developing the Budge-Fudge method of pore pressure estimation, revisited in Part 2. The logs were edited and data points from sandy intervals were removed using the natural gamma log as a discriminator. Sandy samples are deemed to be those with natural gamma values less than 85% of the mean value over the working interval, a criterion that was chosen specifically for this dataset.

Wireline log responses for well 6406/2-5, one of the wells where the Cretaceous mudstones have high porosity (Fig. 2b), are shown in Fig. 7 with two sonic–density crossplots. The mudstone data points on the density and sonic logs (Fig. 7b and e) were smoothed with a Hanning (cosine-bell) window of length 100 m before crossplotting, to reduce scatter on the plot. From a depth of around 2750 m below seafloor, the sonic–density crossplot trend in Fig. 7g parallels Dutta's trend for illite-rich mudstones. At about 3150 m below seafloor, the trend abruptly turns upwards, indicating that unloading of the mudstones accompanies ongoing compaction (cf. Fig. 6), although there are considerable lateral fluctuations that we attribute to lithological variation.

The correlation between sonic transit time and clay content is evident on Fig. 7a, d and e, where fluctuations of about 70 m wavelength can be seen clearly over the interval at 3750–4250 m depth below seafloor. We corrected the sonic log for clay content by making use of the gamma-ray log (Fig. 7a) and values of NPHI – DPHI, the difference between neutron porosity (NPHI) and density porosity (DPHI) (Fig. 7d). The gamma-ray and NPHI – DPHI logs were smoothed using the same Hanning window of length 100 m. Deviations from their respective smoothed trends were calculated for sonic, gamma, and NPHI – DPHI logs. Multipliers for the gamma-ray and NPHI – DPHI deviations were found by simultaneous least squares to obtain the best fit to the sonic log deviations, assuming that the dependence is linear. The mean values of the gamma-ray and NPHI – DPHI log responses were calculated for the mudstones over the whole interval comprising the Kvitnos and Lange formations. Corrections for the sonic log were calculated by subtracting the mean

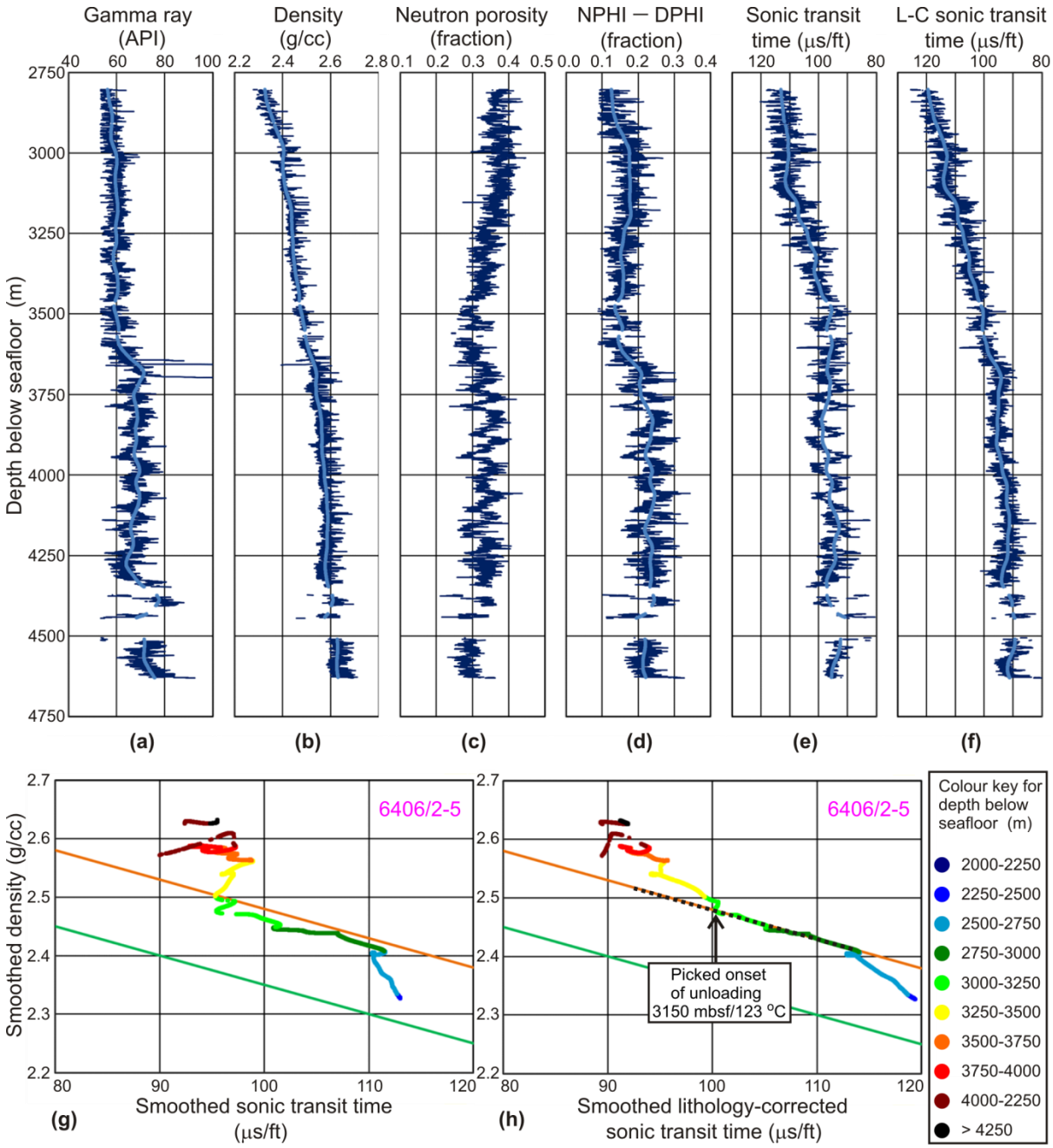

Fig. 7. Wireline logs and derivatives for well 6406/2-5: (a) gamma ray; (b) density; (c) neutron; (d) difference between neutron porosity and density porosity; (e) sonic; and (f) sonic with lithology corrections derived from gamma and NPHI – DPHI values. DPHI was calculated from the density log using 2.75 g cm^{-3} for the density of the solid grains and 1.05 g cm^{-3} for the pore fluid. Smoothed curves using a Hanning window of 100 m length are superimposed in light blue on the logs in (a), (b) and (d) – (f). (g) Sonic–density crossplot for smoothed logs. (h) Sonic–density crossplot using lithology-corrected sonic transit times and smoothed logs. The dotted line is the picked trend for illite-rich mudstones without unloading.

from each of the gamma-ray and NPHI – DPHI logs, and then applying the respective multiplier. The resulting correction terms were subtracted from the sonic transit time at each value of depth (Fig. 7f). The crossplot (Fig. 7h) now shows a more consistent unloading trend, albeit some fluctuations remain. This lithology-correction technique for the sonic log should suppress its sensitivity to clay content without affecting its sensitivity to porosity and effective stress. The onset of unloading is picked at 3150 m depth below seafloor, where the temperature is 123 ^{o}C.

Following the same procedure, sonic–density crossplots for the other nine wells were generated, with lithology corrections applied to the sonic log (Fig. 8). In each case, the onset of the unloading trend was picked and the corresponding depth and temperature are annotated on the plot. To estimate temperatures, geothermal gradients were taken from Cicchino et al. (2015), who calculated them from drill-stem test temperatures, with lateral interpolation where necessary.

3.3. Mechanisms of overpressure generation

Our interpretation of the crossplots in Figs 7h and 8 is as follows. Pore pressure in the Cretaceous formations was close to hydrostatic immediately prior to Naust burial, as suggested by Skar et al. (1999) and O'Connor et al. (2012), although it is possible that there may have been a few megapascals of overpressure, primarily generated by clay diagenesis, especially in the more distal wells in the southwest of the area. Naust burial was especially rapid between 2.8 Ma and 1.5 Ma when the bulk of the Naust Formation was deposited (Rise et al., 2006). Very little pore water could escape from the more distally located Cretaceous mudstones during rapid burial, so mudstone compaction was limited. Warming as a result of increased burial triggered further clay diagenesis that unloaded the Cretaceous mudstones as the normal compaction curve shifted to lower porosity for a given value of vertical effective stress (Lahann, 2002).

In the northeast, the Cretaceous mudstones were better able to drain immediately following rapid Naust burial, so the amounts of overpressure generated at first were much less. Subsequently, the mudstones became sealed as their permeability reduced in response to the additional

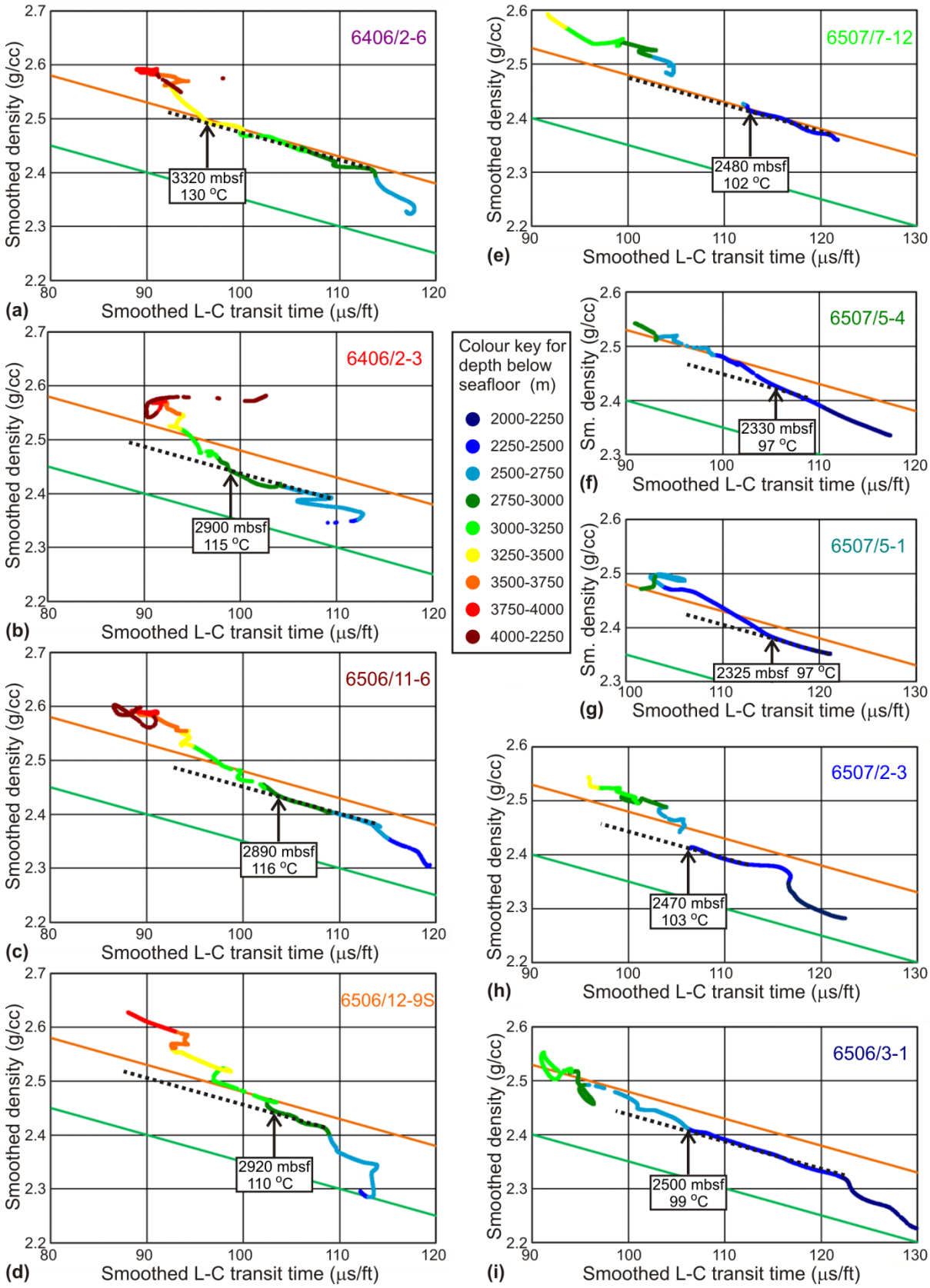

Fig. 8. Sonic–density crossplots for nine more Haltenbanken wells (locations shown in Fig. 2b) using lithology-corrected sonic transit times and smoothed logs. Vertical arrows mark picked onsets of unloading in each well.

mechanical compaction and chemical compaction associated with clay diagenesis, and the pore pressure–depth profile became more uniform across the study area by local lateral transfer. Because of the better drainage in the northeastern wells, the amount of unloading overpressure there, generated by clay diagenesis and local lateral transfer, is relatively large. Consequently, the depths to the onsets of unloading in the northeastern wells are shallower than in the distal wells to the southwest (Fig. 8).

To show that this interpretation of the recent overpressure history is plausible, pressure–depth profiles based on pressure measurements in all ten wells are shown in Fig. 9. In each well, the vertical effective stress is presently the greatest it has ever been in the beds above the onset of unloading, provided that the onset has been picked correctly. The short segment of dotted blue line for each well in Fig. 9 indicates the possible pressure–depth profile immediately following rapid Naust burial, if we make the simplifying assumptions that the rapid burial generated a constant amount of overpressure within each well due to disequilibrium compaction, and that subsequently the pressure–depth profiles adjusted by local lateral transfer with ongoing clay diagenesis and limited drainage.

Assuming perfect sealing of the Cretaceous mudstones, deposition of the Naust would have increased the vertical stress acting on the Cretaceous mudstones and the pore pressure within them by the additional overburden stress at the base of the Naust. At the same time, hydrostatic pressure in the Cretaceous mudstones would have increased by the same amount as the increase in hydrostatic pressure at the base of the Naust. Given that the pore pressure is hydrostatic throughout the Naust, the maximum amount of disequilibrium compaction overpressure that could have been generated by Naust deposition equals the current vertical effective stress at the base of the Naust Formation. However, the values of overpressure at the depths of onset of unloading in wells 6406/2-6, 6406/2-5, 6406/2-3 and 6506/11-6 are larger than the respective values of vertical effective stress at base Naust (Table 1), calculated from density data. There are two possible reasons for these discrepancies. The depths to the onset of unloading may be overestimated,

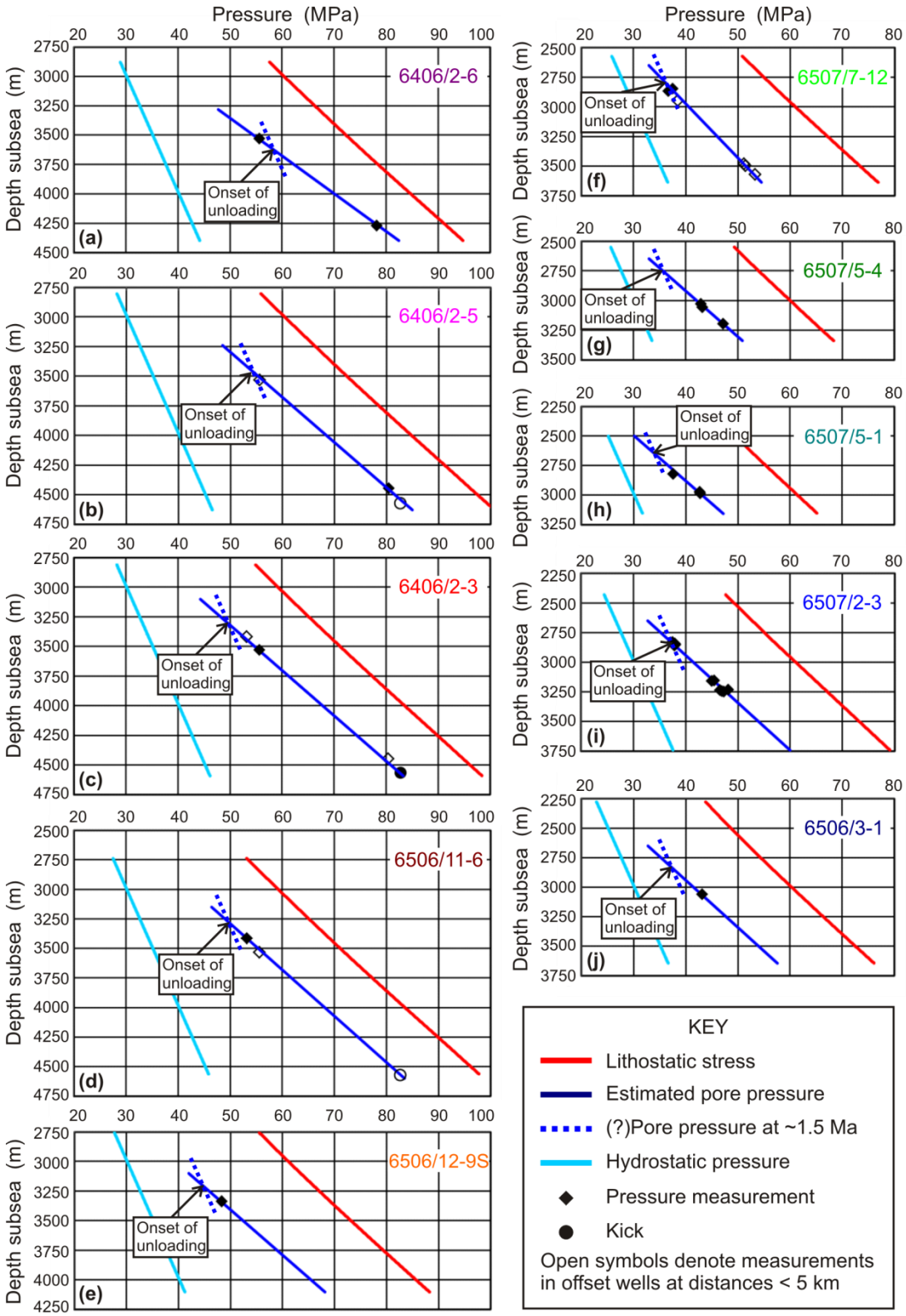

Fig. 9. Pressure–depth profiles within the Cretaceous strata for all ten wells (locations shown in Fig. 2b). Depths are relative to mean sea level. Trends were estimated by fitting to direct measurements of pore pressure, matching the pressure gradient in neighbouring wells where a well contains only a single pressure value. The depths of unloading were picked on the sonic–density crossplots in Figs 7h and 8.

Well no.	Water depth (m)	Kvitnos–Lange interval (mbsf)	Onset of unloading				Vertical effective stress at base Naust (MPa)
			Depth (mbsf)	Temperature (^{o}C)	Vertical effective stress (MPa)	Overpressure (MPa)	
6406/2-6	302	2577 – 4094	3320	130	16.9	22.0	14.6
6406/2-5	341	2462 – 4289	3145	123	14.7	19.9	13.5
6406/2-3	372	2442 – 4220	2900	115	16.9	15.9	12.9
6506/11-6	380	2356 – 4219	2890	116	16.1	16.6	12.7
6506/12-9S	294	2440 – 3787	2920	110	21.2	12.7	12.8
6507/7-12	333	2240 – 3453	2480	102	19.9	8.3	13.0
6507/5-4	421	2130 – 2918	2330	97	18.4	7.9	10.8
6507/5-1	323	2175 – 2831	2325	97	18.9	7.4	11.8
6507/2-3	355	2075 – 3413	2470	103	19.7	8.7	11.3
6506/3-1	341	1936 – TD	2500	99	19.0	9.0	12.9

Table 1 Data from the ten wells used in this study with estimated parameters at the depths of onset of unloading. The vertical effective stress at the base of the Naust Formation equals the maximum possible overpressure generated by disequilibrium compaction as a result of Naust deposition.

because the initial effect on velocity of a reduction in vertical effective stress is small, and there may have been some overpressure present in the Cretaceous mudstones in these four distal wells when Naust deposition began. For the fifth well where the Cretaceous mudstones have high porosity, 6506/12-9S, the overpressure at the onset of unloading approximately equals the vertical effective stress at base Naust. In each of the other five wells, where the Cretaceous mudstones have low porosity, the overpressure at the onset of unloading is less than the vertical effective stress at base Naust, so the vertical effective stress at the present day is greater than it was when Naust deposition began.

4. Compaction processes

In this section, we describe the implications for compaction processes of the differences in vertical effective stress history between the southwestern and northeastern wells. At temperatures above ~100 °C and depths greater that ~2500 m below seafloor, the Cretaceous mudstones have higher porosities in the southwest of the study area and lower porosities in the northeast. The low-porosity mudstones in the northeast have density–depth profiles that are approximately on trend with Hansen's (1996) linear normal compaction trend for hydrostatically pressured mudstones, which suggests that they are close to being fully compacted for their depths of burial (Cicchino et al., 2015).

Hansen's (1996) normal compaction trend is the best available estimate of the maximum amount of compaction in the Cretaceous mudstones for their burial depths at 2.8 Ma, immediately prior to Naust deposition. We infer by the following reasoning that the high-porosity mudstones in the southwest have since become further compacted as a result of clay diagenesis. The density–depth profiles for the high-porosity mudstones in the southwestern wells can be matched to those of the low-porosity wells and to Hansen's (1996) normal compaction trend by an upward shift of just 300–400 m. However, they have been buried by ~1200 m of Naust sediment, so their present-day porosity is less than it was at 2.8 Ma, at the onset of Naust burial, even if the pore pressure was

hydrostatic at that time. Furthermore, analysis of the depths of onset of unloading (Figs 8 and 9 and Table 1) suggests that there may have been a few megapascals of overpressure in the Cretaceous mudstones penetrated by the southwestern wells at 2.8 Ma, so their porosity at that time might have been greater than defined by Hansen's (1996) normal compaction trend. The additional compaction that has taken place since 2.8 Ma must be mainly chemical compaction because the vertical effective stress in the Cretaceous mudstones above the onset of unloading at the present day is the maximum vertical effective stress that those mudstones have experienced, and is less than the vertical effective stress would have been in the same beds prior to Naust burial if the pore pressure had then been hydrostatic.

The depths to the onset of unloading picked on sonic–density crossplots for the northeastern wells confirm that the low-porosity mudstones have been unloaded from vertical effective stress values closer to those corresponding to hydrostatic pore pressure at the present day (Figs 8 and 9). Thus, in the northeast, less of the overpressure generated by rapid Naust burial was retained. The pressure–depth profile is very similar in all Cretaceous mudstones across Haltenbanken, so at any given depth proportionately more of the present-day overpressure in the low-porosity mudstones was generated by unloading processes. In short, mudstones in the northeastern wells have lower porosity than those in the southeastern wells, and have experienced greater vertical effective stress in the past. We conclude that their lower porosity is mainly due to a greater amount of mechanical compaction.

These observations contradict the conceptual model of Bjørlykke and Høeg (1997) and Bjørlykke (1998), in which compaction is expected to be independent of effective stress at temperatures above 100 ^{o}C. The density–depth trends for mudstones in Fig. 5a differ between the southwestern and northeastern wells in the study area throughout their common depth range, down to 3250 m below seafloor (~130 ^{o}C). We attribute the differences primarily to additional mechanical compaction of the low-porosity mudstones in the northeastern wells, and that is entirely

consistent with the Dutta–Lahann model, in which both mechanical and chemical compaction take place in diagenetically altered mudstones above 100 ^{o}C (Dutta, 2002; Lahann, 2002).

5. Discussion and conclusion

Previous studies have observed the lack of a relationship between porosity and effective stress in mudstones buried into the diagenetic regime (e.g., Hermanrud et al. 1998; Teige et al. 1999). Others have reported density increases in mudstones that are not related to effective stress but are coincident with smectite-to-illite transformation (e.g., Peltonen et al. 2009; Lahann and Swarbrick, 2011), which confirms that chemical compaction may take place in association with clay diagenesis.

Hermanrud et al. (1998) found consistent bulk porosities, as inferred from density and neutron logs, in Jurassic intra-reservoir mudstone formations at Haltenbanken where the pore pressure ranged from hydrostatic to high overpressure. They suggested that the reason might be because mudstone compaction had proceeded independently of effective stress, but recognized that a plausible alternative interpretation is that the presence of high pore pressures in association with low mudstone porosities could be a consequence of unloading processes generating overpressure after the mudstones were compacted.

Complementing the observations of Hermanrud et al. (1998), Cicchino et al. (2015) found that porosities in Cretaceous mudstones at Haltenbanken vary by a factor of two at a common depth of 2700 m below seafloor even though the pressure–depth profile is laterally consistent across the area. They pointed out that although clay mineral transformations, such as smectite-to-illite and kaolin-to-illite, take place independently of effective stress, chemical compaction cannot be independent of effective stress. Like mechanical compaction, chemical compaction requires expulsion of pore water; and if expulsion is inhibited, more of the overburden load is transferred to the pore water as overpressure.

The evidence presented here shows that the siliciclastic mudstones of the Cretaceous Lange and Kvitnos formations at Haltenbanken continue to compact mechanically in response to increasing effective stress up to at least 130 ^{o}C. The trends in Fig. 5a are still clearly separated at that temperature, even though they do converge slowly as they approach irreducible porosity. We suggest that the reason why mechanical compaction continues to be viable in these diagenetically altered mudstones is because grain contacts are still predominantly clay–clay contacts following smectite-to-illite transformation.

Acknowledgements

These investigations were carried out as part of the GeoPOP3 project funded by BG, BP, Chevron, ConocoPhillips, DONG Energy, E.ON, ENI, Petrobras, Petronas, Statoil, Total and Tullow. Data were supplied by the Norwegian Petroleum Directorate. We thank Keith Katahara and Rick Lahann for constructive reviews.

References

Bjørlykke, K., 1998. Clay mineral diagenesis in sedimentary basins – a key to the prediction of rock properties: examples from the North Sea Basin. Clay Minerals, 33, 15–34.

Bjørlykke, K., Høeg, K., 1997. Effects of burial diagenesis on stress, compaction and fluid flow in sedimentary basins. Marine and Petroleum Geology, 14, 267–276.

Blystad, P., Brekke, H., Færseth, R.B., Larsen, B.T., Skogseid, J., Tørudbakken, B., 1995. Structural elements of the Norwegian Continental Shelf. Part 2. The Norwegian Sea Region. Norwegian Petroleum Directorate Bulletin, 8, 1–45.

Boles, J.R., Franks, S.G., 1979. Clay diagenesis in Wilcox Sandstones of southwest Texas: implications of smectite diagenesis on sandstone cementation. Journal of Sedimentary Petrology, 49, 55–70.

Bowers, G.L., 2001. Determining an appropriate pore-pressure estimation strategy. OTC 13042.

Bowers, G.L., Katsube, T.J., 2002. The role of shale pore structure on the sensitivity of wireline logs to overpressure. In: Huffman, A.R., Bowers, G.L. (Eds.), Pressure Regimes in Sedimentary Basins and their Prediction. AAPG, Tulsa, 43–60.

Cicchino, A.M.P., Sargent, C., Goulty N.R., Ramdhan, A.M., 2015. Regional variation in Cretaceous mudstone compaction trends across Haltenbanken, offshore mid-Norway. Petroleum Geoscience, 21, 17–34.

Dalland, A., Augedahl, H.O., Bomstad, K., Ofstad, K., 1988. The post-Triassic succession of the Mid-Norwegian Shelf. In: Dalland, A., Worsley, D., Ofstad, K. (Eds.), A lithostratigraphic scheme for the Mesozoic and Cenozoic succession offshore mid- and northern Norway. Norwegian Petroleum Directorate Bulletin, 4, 5–42.

Dowdeswell, J.A., Ottesen, D., Rise, L., 2010. Rates of sediment delivery from the Fennoscandian Ice Sheet through an ice age. Geology, 38, 3–6.

Dutta, N.C., 1986. Shale compaction, burial diagenesis and geopressures: a dynamic model, solution and some results. In: Burrus, J. (Ed.), Thermal Modeling in Sedimentary Basins. Éditions Technip, Paris, 149–172.

Dutta, N.C., 2002. Deepwater geohazard prediction using prestack inversion of large offset P-wave data and rock model. The Leading Edge, 21, 193–198.

Freed, R.L., Peacor, D.R., 1989. Geopressured shale and sealing effect of smectite to illite transition. AAPG Bulletin, 73, 1223–1232.

Gardner, G.H.F., Gardner, L.W., Gregory, A.R., 1974. Formation velocity and density – the diagnostic basics for stratigraphic traps. Geophysics, 39, 770–780.

Giorgetti, G., Mata, P., Peacor, D.R., 2000. TEM study of the mechanism of transformation of detrital kaolinite and muscovite to illite/smectite in sediments of the Salton Sea Geothermal Field. European Journal of Mineralogy, 12, 923–934.

Goulty, N.R., Sargent, C., 2016. Compaction of diagenetically altered mudstones – Part 2: Implications for pore pressure estimation. Marine and Petroleum Geology, in press.

Hansen, S., 1996. A compaction trend for Cretaceous and Tertiary shales on the Norwegian Shelf based on sonic transit times. Petroleum Geoscience, 2, 159–166.

Hermanrud, C., Wensas, L., Teige, G.M.G., Nordgård Bolås, H.M., Hansen, S., Vik, E., 1998. Shale porosities from well logs on Haltenbanken (offshore mid-Norway) show no influence of overpressuring. In: Law, B.E., Ulmishek, G.F., Slavin V.I. (Eds.), Abnormal Pressures in Hydrocarbon Environments. AAPG, Tulsa, 65–85.

Hower, J., Eslinger, E.V., Hower, M.E., Perry, E.A., 1976. Mechanism of burial metamorphism of argillaceous sediment: 1. Mineralogical and chemical evidence. Geological Society of America Bulletin, 87, 725–737.

Katahara, K., 2003. Analysis of overpressure on the Gulf of Mexico Shelf. OTC 15293.

Katahara, K., 2006. Overpressure and shale properties: stress unloading or smectite–illite transformation? SEG Annual Meeting, Expanded Abstracts, 1520–1524.

Lahann, R., 2002. Impact of smectite diagenesis on compaction modelling and compaction equilibrium. In: Huffman, A.R., Bowers, G.L. (Eds.), Pressure Regimes in Sedimentary Basins and their Prediction. AAPG, Tulsa, 61–72.

Lahann, R.W., Swarbrick, R.E., 2011. Overpressure generation by load transfer following shale framework weakening due to smectite diagenesis. Geofluids, 11, 362–375.

Milliken, K.L., 1992. Chemical behavior of detrital feldspars in mudrocks versus sandstones, Frio Formation (Oligocene), South Texas. Journal of Sedimentary Petrology, 62, 790–801.

Nadeau, P.H., 2011. Earth's energy ''Golden Zone'': a synthesis from mineralogical research. Clay Minerals, 46, 1–24.

Nadeau, P.H., Peacor, D.R., Yan, J., Hillier, S., 2002. I–S precipitation in pore space as the cause of geopressuring in Mesozoic mudstones, Egersund Basin, Norwegian continental shelf. American Mineralogist, 87, 1580–1589.

O'Connor, S., Lahann, R., Swarbrick, R., Clegg, P., Kelly, P., Long, J., Diaz, M., Labrum, R., 2012. Mid-Norway Pressure Study. 2nd edn., Ikon GeoPressure, Durham and IHS, Tetbury.

Ottesen, D., Rise, L., Andersen, E.S., Bugge, T., Eidvin, T., 2009. Geological evolution of the Norwegian continental shelf between 61°N and 68°N during the last 3 million years. Norwegian Journal of Geology, 89, 251–265.

Peltonen, C., Marcussen, Ø., Bjørlykke, K., Jahren, J., 2009. Clay mineral diagenesis and quartz cementation in mudstones: the effects of smectite to illite reaction on rock properties. Marine and Petroleum Geology, 26, 887–898.

Rise, L., Ottesen, D., Berg, K., Lindin, E. [2005] Large scale development of the mid-Norwegian margin during the last 3 million years. Marine and Petroleum Geology, 22, 33–44.

Rise, L., Ottesen, D., Longva, O., Solheim, A., Andersen, E.S., Ayers, S., 2006. The Sklinnadjupet slide and its relation to the Elsterian glaciation on the mid-Norwegian margin. Marine and Petroleum Geology, 23, 569–583.

Sargent, C., Goulty N.R., Cicchino, A.M.P., Ramdhan, A.M., 2015. Budge-Fudge method of pore-pressure estimation from wireline logs with application to Cretaceous mudstones at Haltenbanken. Petroleum Geoscience, 21, 219–232.

Schieber, J., 1998. Deposition of mudstones and shales: overview, problems, and challenges. In: Schieber, J., Zimmerle, W., Sethi, P. (Eds.), Shales and Mudstones (Vol. 1): Basin Studies, Sedimentology and Paleontology. Schweizerbart'sche Verlagsbuchhandlung, Stuttgart, 131–146

Skar, T., Van Balen, R.T., Arnesen, L., Cloetingh, S., 1999. Origin of overpressures on the Halten Terrace, offshore mid-Norway: the potential role of mechanical compaction, pressure transfer and stress. In: Aplin, A.C., Fleet, A.J., Macquaker, J.H.S. (Eds.), Muds and Mudstones: Physical and Fluid Flow Properties. Geological Society of London, 137–156.

Środoń, J., Eberl, D.D., Drits, V.A., 2000. Evolution of fundamental-particle size during illitization of smectite and implications for reaction mechanism. Clays and Clay Minerals, 48, 446–458.

Teige, G.M.G., Hermanrud, C., Wensaas, L., Nordgård Bolås, H.M., 1999. The lack of relationship between overpressure and porosity in North Sea and Haltenbanken shales. Marine and Petroleum Geology, 16, 321–335.

Thyberg, B., Jahren, J., 2011. Quartz cementation in mudstones: sheet-like quartz cement from clay mineral reactions during burial. Petroleum Geoscience, 17, 53–63.